Creep Damage Evolution Process of Asphalt Binder Based On Viscoelastic Characteristics

Tian Shuang
Shihezi University
QI Xiaofei
Harbin Institute of Technology
shan liyan (myshanliyan@126.com)
Harbin Institute of Technology
Liu Shuang
Harbin Institute of Technology
Wang Yajie
Harbin Institute of Technology

Research

Keywords: asphalt binder, multi-stage creep test, damage variable, evolution law

Posted Date: April 28th, 2021

DOI: https://doi.org/10.21203/rs.3.rs-437109/v1

Creep Damage Evolution process of Asphalt Binder Based on Viscoelastic Characteristics

Shuang Tian [a], Xiaofei Qi [b], Liyan Shan[b*], Shuang Liu [b] , Yajie Wang [b]

[a] School of Water and Architectural Engineering, Shihezi University, Shihezi, Xinjiang 832003, China;

[b] School of Transportation Science and Engineering, Harbin Institute of Technology, Harbin, Heilongjiang150090, China.

Abstract: The creep damage evolution of asphalt binder plays a significant role in investigating the formation mechanism of rutting, a common type of distress at high temperature for asphalt pavements. However, the reliability of existing creep damage parameters is under questioned, and these parameters cannot accurately illustrate change law of intrinsic microstructure about asphalt binder. In this paper, a new testing protocol is given access to study the evolution of viscoelastic parameters during creep damage. It is completed by inserting the frequency sweep during creep test. The frequency sweep curve clusters are fitted using the generalized Kelvin-Voigt model for obtaining the change law of model parameters. Based on the change law and sensitivity analysis of model parameters, $(E_2+E_3)/2$ is proposed as the creep damage variable. According to the curve of $(E_2+E_3)/2$ versus loading time, two stages during the creep test can be identified: an approximate constant value in phase I and a linear decrease in phase II. Intrinsic differences about creep property of binders can be determined by this new proposed parameter. Above results not only ensure better understanding of the creep damage mechanism of binders, but also lay the theoretical foundation on predicting the anti-rutting performance of binders.

Key words: asphalt binder, multi-stage creep test, damage variable, evolution law.

1. Introduction

Rutting is a common deterioration observed in asphalt pavement during hot reasons. It appears in the form of longitudinal depression along the wheel path under repetitive traffic loads. [1]. Asphalt binder, as an important part of pavement material, the high temperature performance of which has a profound effect on the rutting susceptibility of asphalt pavement. Thus, much research had been performed to investigate the anti-rutting performance of asphalt binders over the past few decades [2-4].

Among the various evaluation methods for high temperature property of asphalt binders, the creep test is the most common method [5]. For the steady creep experiment, the stress keeps constant and the strain varies as time. The creep property of binders can be quantified by creep compliance (J(t)), which is the ratio between strain and stress. The larger creep compliance of asphalt binder is, the easier it deforms. For distinguishing recoverable elastic deformation and non-recoverable viscous deformation, Bahia et al. proposed the Repeated Creep Recovery Test (RCRT) to characterize the rutting susceptibility of asphalt binders [6]. The durations of the creep and recovery phases were supposed to be 1 s and 9 s respectively during the RCRT. The ability to resist permanent deformation of binders can be assessed by viscous component of creep stiffness (Gv) using the Burgers model. [7] Besides, the value of accumulated strain at the end of the test was also proposed as the anti-rutting index of binders [8,9]. In order to introduce the nonlinearity associated with asphalt binders and make RCRT more accurate, multiple stress creep and recovery (MSCR) test was proposed by D'Angelo [10]. The creep recovery rate (R) and non-recoverable creep compliance (J_{nr}) are calculated as rutting resistance criterion. The test is composed of creep loading and unloading cycle of 1 s and 9 s respectively at stress levels of 0.1 kPa and 3.2 kPa. Ten cycles of loading are given at each stress level. Various laboratory and field investigations have proved this method to be applicable for both unmodified and modified binders [11-13]. However, these creep

parameters only reflect the macroscopic mechanical behavior of asphalt binders during creep. They could not reveal the damage evolution of intrinsic microstructural attribute of binders under cyclic loadings.

The researchers had done a significant amount of work about damage parameters using modulus, dissipated energy and other damage evolution functions, such as Weibull function et al. [14-16] However, above damage parameters defined are of average meaning and cannot truly describe topo-damage evolution of asphalt binders. As a typical viscoelastic material, asphalt binder can be approximately equivalent to a kind of composite. It can be made up by springs and dashpots in series or in parallel. Namely, the elements representing for different viscoelastic model parameters. These parameters can reflect different microstructural properties of asphalt binders [17]. Based on this characteristic, some researchers start to study new damage evaluate scheme combined with viscoelastic model parameters. It can contribute to precisely analyze the damage evolution of asphalt binders. Rompu et al. [18] had designed an advanced fatigue test referenced to above theory and established fatigue damage evolution of asphalt binders by the 1S2P1D viscoelastic parameters. However, this method has not still been applied on analyzing the creep damage evolution of asphalt binders.

In this paper, the main objective is to investigate the creep damage evolution of asphalt binders based on viscoelastic parameters. For this purpose, the multi-stage creep test was presented in this work, including the description of the testing procedures and tested materials. Secondly, the frequency sweep curve clusters of asphalt binders at different test points were plotted. The next part was devoted to the model, including the model principle and optimization method. Then, the fitting results were presented by plotting the evolution of viscoelastic model parameters as function of loading time. Finally, based on the sensitivity analysis about these fitting parameters, the creep damage

variable and the damage evolution law of binders were determined in the study.

2. Materials and methods

2.1 Materials

Two neat asphalt binders were selected for this study and they were unified as binder A and binder B. Specifically, the penetration grade of binder A is 60–80, the penetration grade of binder B is 80–100, in accordance with the Chinese penetration grade system. The basic properties of studied asphalt binders are tabulated in Table 1.

Table 1 The basic properties of the studied asphalt binders.

Contents	Unit	Binders	
		A	B
Penetration (100g,25°C，5s)	0.1mm	77.4	94.3
Softening point, $T_{R\&B}$	°C	47.2	46.5
Ductility (15°C)	cm	>100	>100

2.2 Methods

In this study, the stress sweep test, conventional creep test and multistage creep test were conducted using a TA Instruments DHR-2 rheometer. All tests were conducted using a 25-mm parallel plate geometry and a 1-mm gap setting. The tests followed the protocols developed in the previous study. [19] Two replicates were performed for each test in this paper.

2.2.1. Stress sweep test

Prior to conducting creep tests, stress sweep tests were conducted to determine the linear viscoelastic regime of binders. Based on the time-temperature superposition (TTS) principle, it is much easy to achieve the linear critical stress at high temperature and low frequency. For all the following test conditions in this paper, the highest temperature and lowest frequency is 50°C and 5Hz respectively. Therefore, Fig.1 only presents the results of stress sweep tests at 50°C and 5Hz. According to the Strategic Highway Research

Program (SHRP), if the decrease in the dynamic modulus value is less than 10% of the initial modulus value, the binder is believed to be in the linear regime [20]. As shown in Fig.1, the critical stress amplitude of asphalt A is 9300Pa; the critical stress amplitude of asphalt B is 8000Pa. When the applied stresses were lower than the critical stress amplitude under the above test condition for these two binders, all the stress levels for the subsequent tests would be in the linear regime.

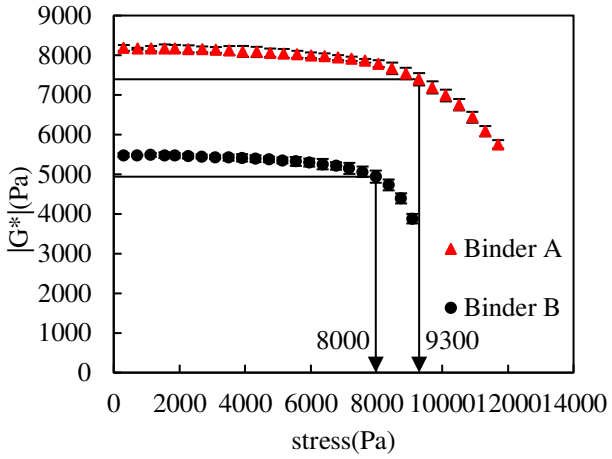

Fig. 1 Stress sweep test results of the asphalt A and B at 50°C,5Hz

2.2.2 Conventional creep test

The conventional creep test could be effectively utilized to evaluate the high temperature performance of asphalt binders. The creep tests of asphalt binders at 40°C and 50°C were carried out in this study. The stress applied to the studied binders was set as 7000Pa at 40°C; the stress applied to the studied binders was set as 3500Pa at 50°C in this paper.

2.2.3 Multi-stage Creep Test

The greatest improvement of this test consists in the insertion of test to measure the linear viscoelastic parameters during creep test. The testing protocol is presented in Fig.2. Assume that the n_{th} creep test time is t_n. The frequency sweep test performed on binders were conducted at the time point. It can contribute to establishing modulus and phase angle curve clusters of asphalt binders. The frequency series were chosen as 5Hz, 10Hz,

15Hz, 20Hz, 30Hz, 40Hz, 60Hz, and all applied stresses were set in the linear regime.

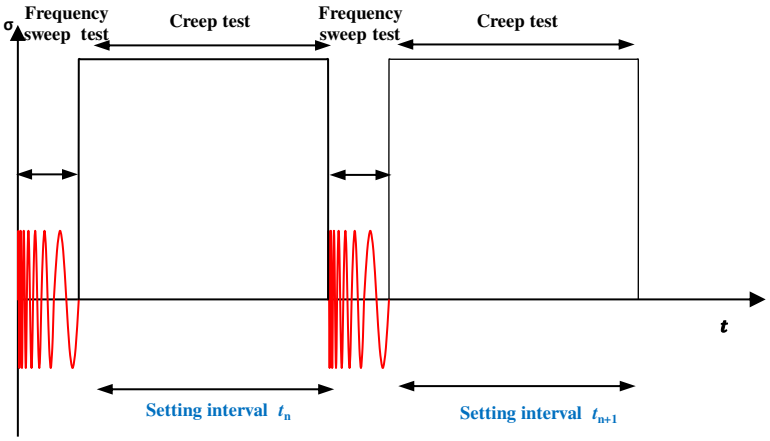

Fig.2 Schematic representation of the multi-stage creep test protocol

In order to verify the feasibility of this method, take asphalt binder A as an example, the comparisons of double-logarithmic curves about creep compliance versus time for conventional creep test and multi-stage creep test are presented in Fig.3. The data of multi-stage creep test is denoted by A_a. As shown in Fig.3, the creep compliance curves of these two test methods are slightly different. This is because of the time interval caused by frequency sweep during multi-stage creep test. Nevertheless, the change trend about creep compliance versus time for these two kinds of tests is similar in general, which validates the reliability of the new designed test. That is, multistage creep test can be used to investigate creep damage evolution law of asphalt binders.

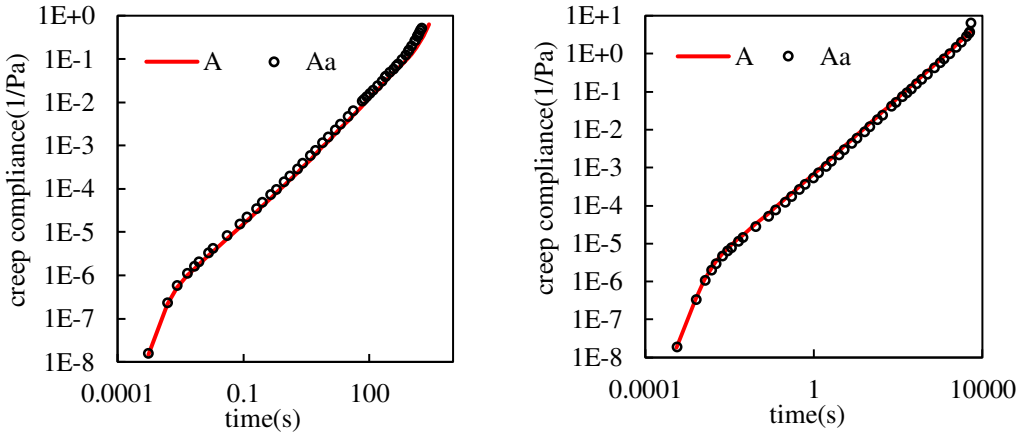

a) A-40°C b) A-50°C

Fig.3 The double-logarithmic curves of creep compliance versus time for conventional creep test and multistage creep test.

3. Results and discussions

3.1 Analysis about conventional creep characteristic parameters of asphalt binders

By the conventional creep tests showed above, the variations of strain and creep compliance versus time for asphalt binder A and B were obtained. The curves of strain versus time for binder A and B at different temperatures were presented in Fig.4. The different test conditions were coded as: asphalt binder type, test temperature such as "A-40" produced with binder A and 40°C. As shown in Fig.4, strain of binders under all testing temperatures linearly increases with the increase of time at the initial stage of loading, and then the growth rate of strain begins to rapidly increase until the specimen is destroyed completely. The growth rate of strain as time of binder B is obviously greater than that of binder A at the same temperature. It means that the time of binder B it takes to reach the same strain is shorter than that of binder A. Namely, the deformation resistance of asphalt A is better. Moreover, higher temperature will result in shorter time to reach the same strain, which reflects the temperature dependence of binders.

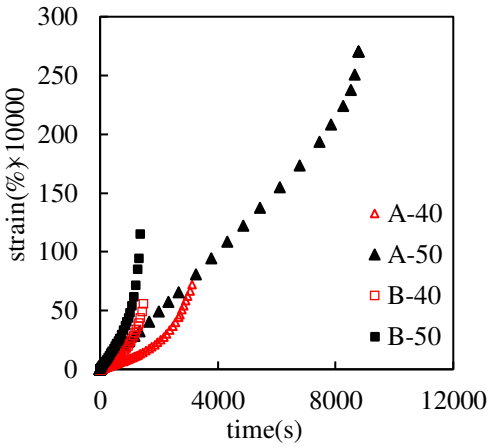

Fig.4 The curves of strain versus time for two asphalt binders.

Fig.5 shows the double-logarithmic curves of creep compliance versus time of binder A and B at different temperatures. As can be seen from Fig.5, the creep compliance

has a rapid increase initially, following by a linear increase, and then sharply increases. Corresponding to the existing research, the three stages are migration creep stage, stable creep stage and accelerated creep stage [21]. The higher the temperature is, the later the first and second stages of creep curves appear. It means that the longer it takes to enter a stable creep state. The lower the temperature is, the smaller the initial creep damage is. Namely, the stronger the anti-deformation ability is. Moreover, the creep compliance of asphalt B is greater than A at the same temperature. It also verifies that the deformation resistance of asphalt A is better.

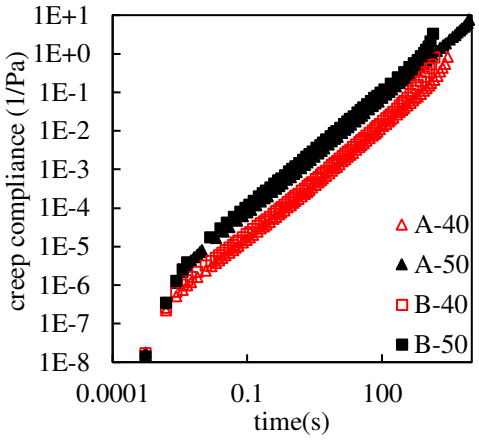

Fig.5 The double-logarithmic curves of creep compliance versus time for two asphalt binders

3.2 Analysis about multi-stage creep test results of asphalt binders

3.2.2 Establishment of curve clusters about viscoelastic parameters

Based on the test data of frequency sweep at different time points, the curve clusters of viscoelastic parameters are shown in Fig.6, only setting the binder A at 40°C as an example.

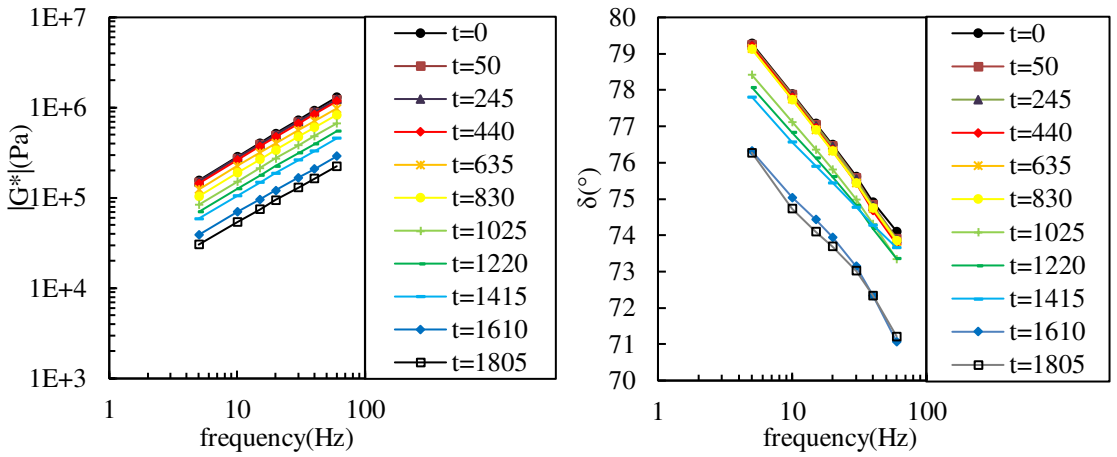

a) complex modulus versus frequency curve b) phase angle versus frequency curve

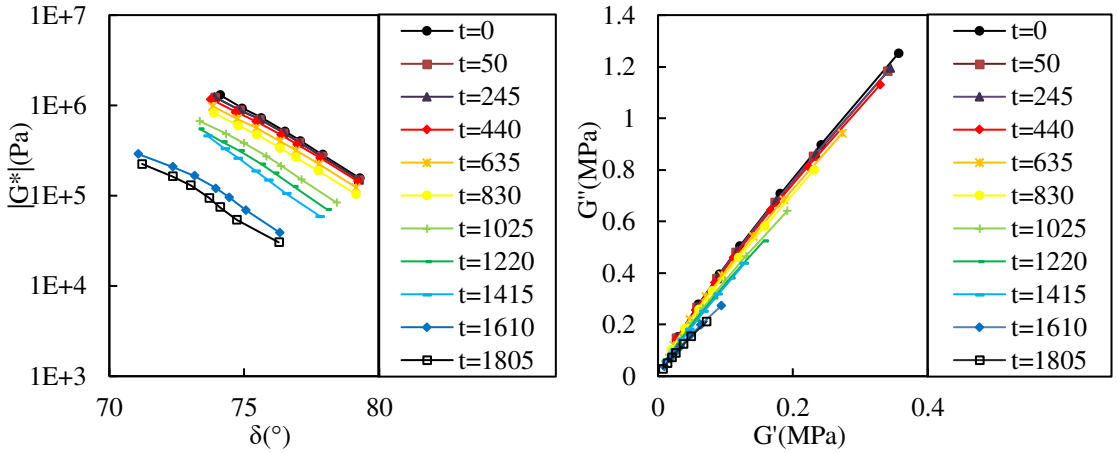

c) complex modulus versus phase angle curve d) loss modulus versus storage modulus curve

Fig.6 The curve clusters of viscoelastic parameters of binder A at 40℃

The curve clusters of complex modulus versus frequency are plotted in Fig.6a, which shows that the complex modulus increases linearly with the increase of frequency. As shown in Fig.6a, the shapes of curve clusters are basically similar during the creep damage process. With the increase of loading time, the complex modulus under all frequencies continually decreases. It means that the internal structure of binder is destroyed during the creep damage. And the gap value of adjacent complex modulus versus frequency curves gradually increases at some extent, which illustrates that the sensitivity of viscoelastic properties obviously increases at the later stage of creep damage for asphalt binder.

The relationship between phase angle and frequency at different time points is plotted in Fig.6b. The change trend of phase angle versus frequency curve clusters is basically consistent and the phase angle decreases linearly with the increase of frequency at early stage of creep test. At late stage of creep test, the phase angle decreases rapidly from slow to fast with the increase of frequency. It greatly deviates from the initial curve clusters in the range of high frequency. And the longer the loading time acts, the greater the phase angle versus frequency curve deviates. It can be concluded that the visco-elastic ratio of asphalt binder is greatly affected by creep damage at the high frequency.

The curve clusters of complex modulus versus phase angle are plotted in Fig.6c. At the beginning of loading time, the curves are basically similar. The complex modulus and phase angle gradually reduce with the increase of creep time, which indicates elastic proportion of binders increases during the creep damage. Moreover, the curves obviously deviate from the parallel line of initial curve clusters at the end of creep test. It means that the change of internal microstructure is different between the beginning and ending of the creep damage about asphalt binder. The gap change of the adjacent curves further illustrates that the viscoelastic sensitivity of asphalt binder gradually increases during the creep damage.

Fig.6d presents the results from the curve clusters of loss modulus versus storage modulus. The length of the curves gradually decreases, and the curves are all arc-shaped. The curve clusters at the initial stage of loading are basically unchanged, while at the later stage, the loss modulus and storage modulus of asphalt binder both show a trend of rapid decrease.

3.3 Damage evolution process of binders based on generalized Kelvin-Voigt viscoelastic model

In this section, the curve of each test time node was fitted by the generalized Kelvin-

Voigt viscoelastic model to obtain the change trends of viscoelastic model parameters.

3.3.1 Presentation of the generalized Kelvin-Voigt model

Considering the fitting accuracy [22], this model is made up of eight Kelvin elements and one Maxwell element in series (as shown in Fig.7).

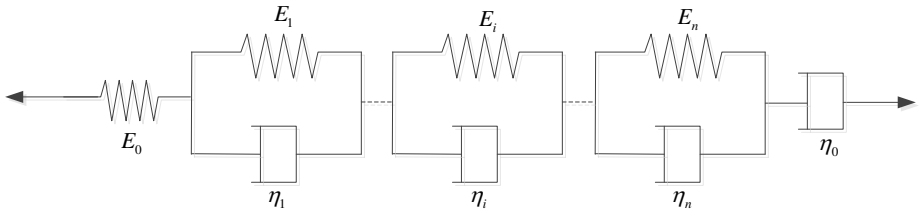

Fig.7 Representation of Generalized Kelvin-Voigt model

The corresponding mathematical equation of the dynamic modulus for the generalized Kelvin-Voigt model is listed in Eq (1).

$$G^*(i\omega)=\frac{1}{(\sum_{i=1}^{8}\frac{E_i}{E_i^2+\eta_i^2\omega^2}+\frac{1}{E_\infty})-(\sum_{i=1}^{8}\frac{\eta_i\omega}{E_i^2+\eta_i^2\omega^2}+\frac{1}{\eta_0\omega})i}=G'(\omega)+G''(\omega)i \quad (1)$$

Where $G^*(i\omega)$ is the complex modulus, Pa; ω is the angular frequency, rad/s; $G'(\omega)$ is the storage modulus, Pa; $G''(\omega)$ is the loss modulus, Pa; E_∞ is elastic modulus of the Maxwell element, Pa; η_0 is the viscosity coefficient of the Maxwell element, $Pa\cdot s$; E_i is the elastic modulus of the i th Kelvin element, Pa; η_i is the viscosity coefficient of the i th Kelvin element, $Pa\cdot s$; τ_i (E_i/η_i) is relaxation time of the i th Kelvin element.

In order to get the obvious changes of model parameters versus the loading time, assuming the value of τ_i based on the frequency range in the curve clusters of asphalt binders in this study [23]. Taking asphalt binder A as an example, the order of frequency magnitude in the master curve ranges from 10^{-6} to 10^{+7}. The values of τ_i (i=1,2,3,4,5,6,7,8) are set as10^{-6},10^{-4},10^{-2},10^{-1},10^{1},10^{2},10^{4} and 10^{7} respectively. There will be only the

226 unknown parameter E_i in the Kelvin elements during the calculated process.

227 The optimization method is to minimize the difference between all the measured
228 results and the corresponding fitted results as shown in Eq(2) by using Solver in Excel
229 [24].

230 $$f_{\min} = \sum_{i=1}^{m} \left(\frac{\left|G'_f - G'_e\right|}{G'_e} + \frac{\left|G''_f - G''_e\right|}{G''_e} + \frac{\left|G^*_f - G^*_e\right|}{G^*_e} + \frac{\left|\delta_f - \delta_e\right|}{\delta_e} \right) \quad (2)$$

231 Where subscript *e* is tested value; subscript *f* is fitted value; *m* is the number of
232 frequency.

233 **3.3.2 Evolutions of the model parameters**

234 According to the above analysis, the fitted results of generalized Kelvin-Voigt model
235 parameters are plotted in Fig.8. Taking binder A at 40°C as an example, evolutions of E_i
236 are plotted in Fig.8(a) as the function of loading time. It shows that the elastic modulus
237 E_i displays different change laws as the loading time increases during the creep damage.
238 E_1, E_6, E_7 and E_8 values fundamentally remain constant as the loading time increases.
239 E_2 and E_3 values keep stable at the beginning of the test, then these two parameters
240 gradually decrease as the loading time increases. E_4 and E_5 values slightly decrease
241 during the whole test, however, the curve presents certain fluctuation at the end of test.
242 Due to the edge effect [24], the accuracy of parameters corresponding to τ_1 is under
243 suspicion. Therefore, the characteristic time of the element which contributes most for
244 the macro-property of asphalt binders is τ_2 (the value is 10^{-4}), that is main relaxation time
245 of asphalt binders.

246 The elastic modulus of the Maxwell element (E_∞) remain foundationally constant
247 as the loading time increases for each measurement, as illustrated in Fig.6(b).
248 Nevertheless, the order of magnitude of E_∞ value is 3-4 orders larger than that of E_2

value corresponding to the main relaxation time. It might be related to the form of degraded dashpot in series.

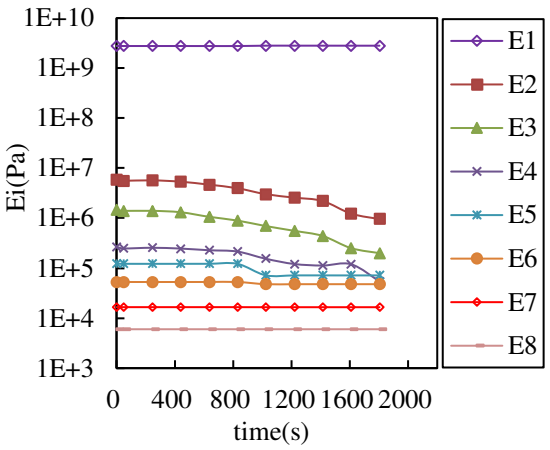

(a) E_i plotted as a function of the loading time

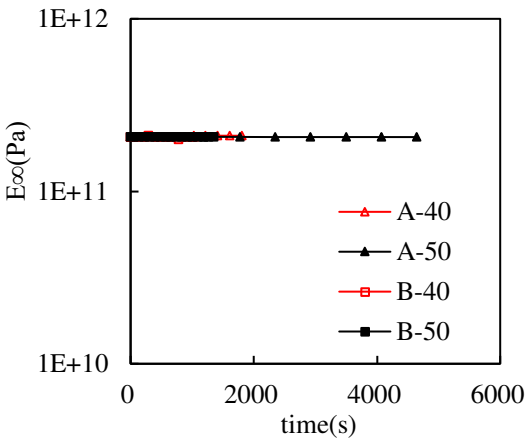

(b) E_∞ plotted as a function of the loading time

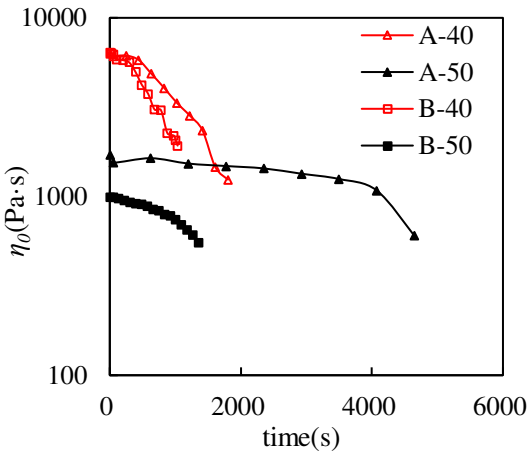

(c) η_0 plotted as a function of the loading time

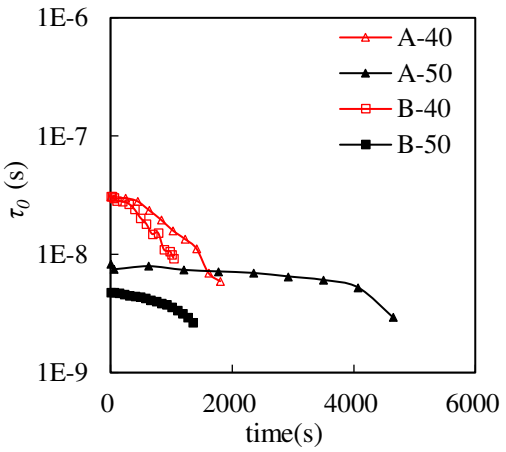

(d) τ_0 plotted as a function of the loading time

Fig.8 Parameters of the generalized Kelvin-Voigt model plotted as a function of the loading time during multi-stage creep test of binder A at 40℃.

Evolutions of η_0 as the function of loading time for all the test conditions are given in Fig.8(c). As can be seen, η_0 value remains constant at the beginning of test, then, this parameter gradually decreases as the loading time increases.

In order to identify the order of magnitude of degraded elements (including spring element and dashpot element) in this paper, the Maxwell element is proposed to replace the two degenerate elements for further analysis. Evolutions of τ_0 (the relaxation time of

263 the supposed Maxwell element) as the function of loading time are given in Fig.8(d). It
264 could be seen that the change of τ_0 versus the loading time is approximately consistent
265 with the change laws of η_0 versus the loading time. For the order of magnitude of τ_0
266 (10^{-9}~10^{-7}), it is far less than the main relaxation time (10^{-4}). It means that this relaxation
267 time point precedes the end effect time point. Thus, the subsequent analysis of damage
268 parameters does not consider the viscoelastic parameters of this element.

269 According to aforementioned analysis, it concluded that the viscoelastic property
270 mainly depends on the parameter E_2, E_3, E_4 and E_5 during the creep damage.

271 **3.4 Analysis of the creep damage evolutions based on damage parameter**

272 **3.4.1 Identification of damage variable**

273 In order to identify the creep damage variable, the sensitivity of viscoelastic
274 characteristic parameters E_i of the generalized Kelvin-Voigt viscoelastic model was
275 studied using the mean square deviation in this section. The calculated results are
276 available in Table 2. It could be seen that the mean square deviations of E_2 and E_3 are
277 obvious higher than that of other parameters under all test schemes. Besides, the
278 sensitivity values of these two parameters are basically uniform for each test. Thus,
279 $(E_2 + E_3)/2$ is proposed as the creep damage variable in the paper.

280 Table 2 Sensitivity analysis results of E_i

σ	E_1	E_2	E_3	E_4	E_5	E_6	E_7	E_8
A-40	0.004	0.275	0.307	0.218	0.121	0.023	0.001	0.000
A-50	0.000	0.145	0.167	0.090	0.003	0.001	0.000	0.000
B-40	0.005	0.182	0.190	0.160	0.003	0.001	0.000	0.000
B-50	0.000	0.085	0.085	0.045	0.000	0.000	0.000	0.000

281 **3.4.2 Analysis of creep damage evolution**

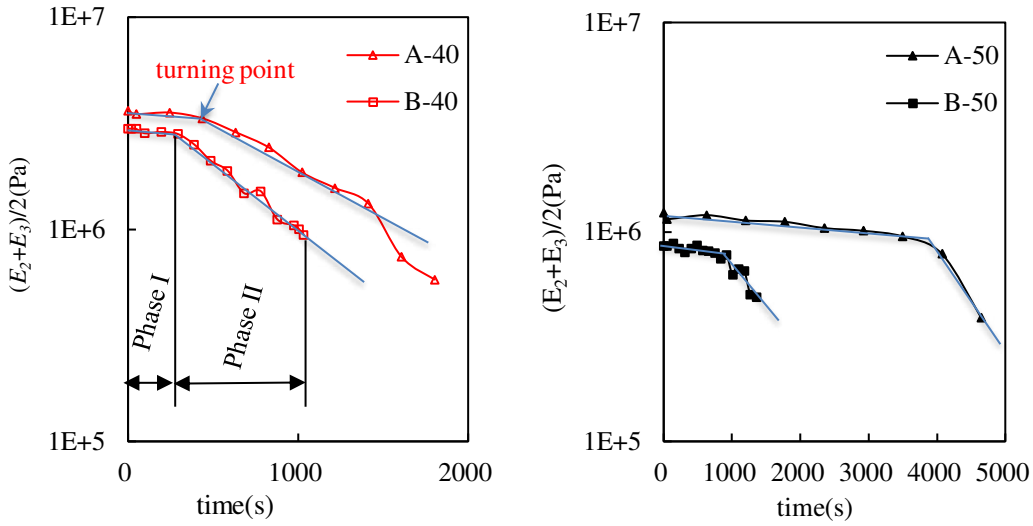

(a) Creep damage evolutions at 40°C (b) Creep damage evolutions at 50°C

Fig.11 Damage parameter $(E_2+E_3)/2$ plotted as the function of loading time during multi-creep test

The evolutions of $(E_2+E_3)/2$ are plotted as the function of loading time during the multi-creep test in Fig.11. As described in Fig.11, the shape of $(E_2+E_3)/2$ versus loading time curve can be obviously divided into two stages for each test, including an approximate constant value in phase I and a linear decrease in phase II. The $(E_2+E_3)/2$ value of asphalt binder A is relatively higher compared with asphalt binder B. The turning point between phase I and phase II is obviously later and the curve slop of phase II is higher for asphalt binder A. It means that the asphalt binder A has a good ability of resisting damage. The turning point between phase I and phase II and the curve slope in phase II present obvious distinction under different test conditions. It reflects sensitivity of this parameter to material styles and temperature conditions. Nevertheless, the change law of $(E_2+E_3)/2$ versus loading time for different tested materials and testing temperatures is approximately consistent. It verifies that the reliability of the creep damage variable proposed in this study.

4. Summaries and Conclusions

The aim of this study is to better understand the creep damage evolution of asphalt binder. The advanced multi-creep test was given access to study the evolution of material viscoelastic parameters during creep damage process. The curve clusters of viscoelastic parameters obtained by the multi-creep test were analyzed. The evolutions of model parameters were simulated by the generalized Kelvin-Voigt model. Finally, the creep damage variable was proposed and the creep damage evolution stages were also determined. In the future, more types of asphalt binders would be used to verify the obtained conclusions. Based on the results presented, several conclusions can be concluded:

(1) For the evolution of generalized Kelvin-Voigt model parameters, the viscoelastic behavior mainly depends on the parameters E_2, E_3, E_4 and E_5.

(2) According to the change laws and sensitivity of viscoelastic model parameters, the parameter $(E_2+E_3)/2$ can be proposed as the intrinsic variable of creep damage.

(3) The shape of $(E_2+E_3)/2$ versus loading time curves can be obviously deduced two stages, including an approximate constant value in phase I and a linear decrease in phase II. The analysis of this parameter points out differences between tested materials, verifying the accuracy of the proposed creep damage variable.

Corresponding author E-mail： myshanliyan@126.com

Mailing address： School of Transportation Science and Engineering, Harbin Institute of Technology, 73 Huanghe Road, Nangang District, Harbin City, Heilongjiang Province, China.

Abbreviations

$G^*(i\omega)$:Complex modulus; ω : Angular frequency; $G'(\omega)$:Storage modulus; $G''(\omega)$:Loss modulus; E_∞ :Elastic modulus of the Maxwell element; η_0 : Viscosity

coefficient of the Maxwell element; E_i :Elastic modulus of the i th Kelvin element; η_i :Viscosity coefficient of the ith Kelvin element; τ_i :Relaxation time of the i th Kelvin element; e :Tested value; f: Fitted value; m :Number of frequency

Acknowledgements

This study was sponsored by the National Natural Science Foundation of China (51778195, 51978218).

Authors' contributions

Conceptualization, L.S.; Methodology, L.S., S.T. and X.Q.; Validation, X.Q. and Y.W.; Investigation, X.Q., L.S.; Data curation, S.T., X.Q. and S.L.; Writing-Original Draft Preparation, X.Q.; Writing-Review and Editing, X.Q., S.T. and Y.W.; Supervision, L.S. The authors read and approved the final manuscript.

Funding

This study was sponsored by the National Natural Science Foundation of China (51778195, 51978218).

Availability of data and materials

All data used or generated by this study is available from the corresponding author by reasonable request.

Ethics approval and consent to participate

Not applicable.

Consent for publication

Not applicable.

Competing interests

The authors declare that they have no competing interests.

Author details

[1] School of Water and Architectural Engineering, Shihezi University, Shihezi, Xinjiang

832003, China.[2] School of Transportation Science and Engineering, Harbin Institute of Technology, 73 Huanghe Road, Nangang District, Harbin City, Heilongjiang Province,150090, China.

References

[1] Al-Khateeb G, Shenoy A, Gibson N (2007) Mechanistic performance analyses of the FHWA's accelerated loading facility pavement. J Assoc Asphalt Paving Technol. (AAPT) 76:737–770

[2] Bouldin M, Dongré, R, D'Angelo J (2001) Proposed refinement of Superpave high temperature specification parameter for performance-graded binders. J Transp Res Board 1766:40–47

[3] Dongré R, D'Angelo J (2003) Refinement of Superpave high-temperature binder specification based on pavement performance in the accelerated loading facility. J Transp Res Board 1829: 39–46.

[4] Radhakrishnan V, Ramya Sri M, Sudhakar Reddy K (2018) Evaluation of asphalt binder rutting parameters. Constr Build Mater 173:298-307.

[5] Du Y, Chen J, Han Z, et al (2018) A review on solutions for improving rutting resistance of asphalt pavement and test methods. Constr Build Mater, 168:893-905.

[6] Bahia HU, Zhai H, Zeng M, Hu Y, Turner P (2001) Development of binder specification parameters based on characterization of damage behavior. J Assoc Asphalt Pavement 70:442–470.

[7] Laukkanen, O V , Soenen, H , Pellinen, T, Heyrman, S , Lemoine, G (2014) Creep-recovery behavior of bituminous binders and its relation to asphalt mixture rutting. Materials and Structures 48(12):4039-4053

[8] Merusi F, Giuliani F (2011) Intrinsic resistance to nonreversible deformation in modified asphalt binders and its relation with specification criteria. Constr Build Mater 25:3356–3366

[9] Hrdlicka GM, Tandon V (2007) Estimation of hot-mix asphalt concrete rutting potential from repeated creep binder tests. In: TRB 86th annual meeting, Washington, Paper 07-2886

[10] D'Angelo, J A (2009) The relationship of the MSCR test to rutting. Road Materials and Pavement Design 10 (Sup1):61–80. Taylor & Francis Group

[11] Dubois, E, Mehta, D Y and Nolan A.(2014) Correlation between multiple stress creep recovery (MSCR) results and polymer modification of binder. Constr Build Mater 65:184–90

[12] Saboo, N., and Kumar P. (2016) Analysis of different test methods for quantifying rutting

susceptibility of asphalt binders. J Mater Civil Eng 28 (7):04016024

[13] Yongmei G , Li X U , Liang W U , et al(2018) High-Temperature Performance Evaluation of Modified Asphalts Based on Multiple Stress Creep Recovery Test. Journal of Building Materials

[14] Sullivan R W (2008) Development of a viscoelastic continuum damage model for cyclic loading. Mech Time-Dependent Mat 12(4):329-342

[15] Katsuki D, Gutierrez M (2011) Viscoelastic damage model for asphalt concrete. Acta Geotechnica 6(4):231-241

[16] Darabi M K, Abu Al-Rub R K, Masad E A, et al (2013) Constitutive modeling of fatigue damage response of asphalt concrete materials with consideration of micro-damage healing. Int J of Solids St 50(19):2901-2913

[17] Zeng M, Bahiu H U, Zhai H, et al (2001) Rheological modeling of modified asphalt binders and mixtures. Asphalt Paving Technology: Association of Asphalt Paving Technologists-Proceedings of the Technical Sessions 70(1):403-441

[18] Rompu J V, Benedetto H D, Buannic M, et al (2012) New Fatigue Test On Bituminous Binders: Experimental Results and Modeling. Constr Build Mater 37:197-208

[19] Shan LY, He Hongsen, Wagner NJ, Li Z (2018) Nonlinear rheological behavior of bitumen under LAOS stress. J Rheol 64(2): 975-989

[20] Anderson D. A., Christensen D. W., Bahia H. U., Dongre R., Sharma M. G., and Antle C. E., et al (1994) Binder characterization and evaluation. volume 3: physical characterization. Asphalt Cement

[21] Ye Y, Yang X, Chen C (2009) Experimental researches on visco-elastoplastic constitutive model of asphalt mastic. Constr Build Mater 23(10):3161-3165

[22] Shan L Y, Xu Y, He H S, et al. (2016) Optimization criterion of viscoelastic response model for asphalt binders. Constr Build Mater 113:553-560

[23] Wu Q Y, Wu J A. Polymer Rheology (Second Edition). Beijing: Higher Education Press, 2014:157-165

[24] Shan L Y, Tan Y Q, Zhang H , et al (2016) Analysis of Linear Viscoelastic Response Function Model for Asphalt Binders. J Mater Civil Eng 28(6):04016010

[25] Yin Y M (2011) Research on Dynamic Viscoelastic Characteristics and Shear Modulus Predicting Methods for Asphalt Mixtures Based on DMA Means. Guangzhou, South China

Figures

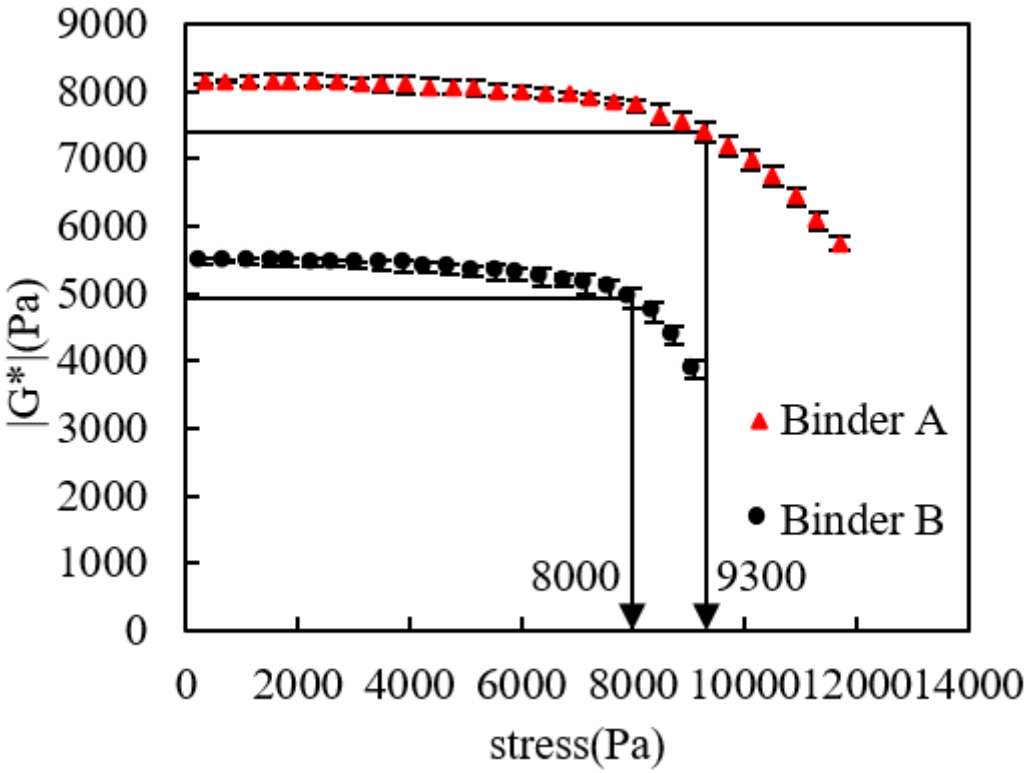

Figure 1

Stress sweep test results of the asphalt A and B at 50℃,5Hz

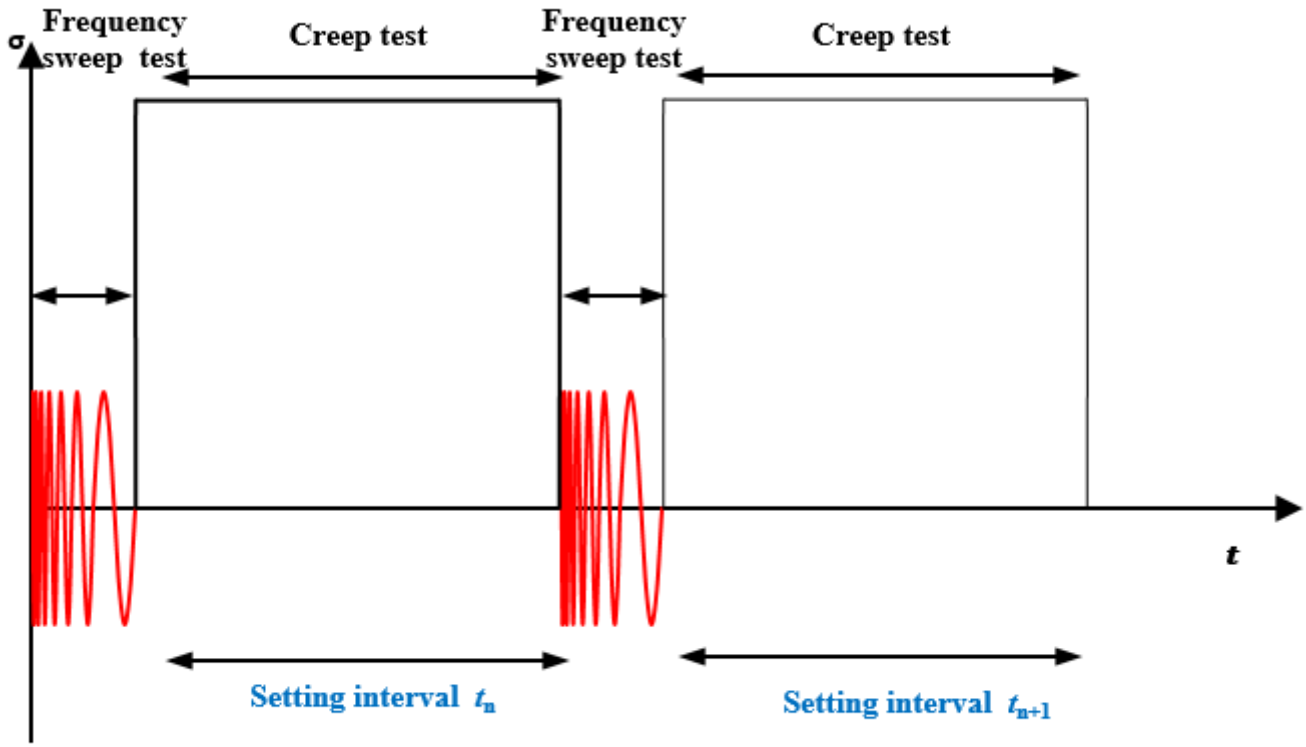

Figure 2

Schematic representation of the multi-stage creep test protocol

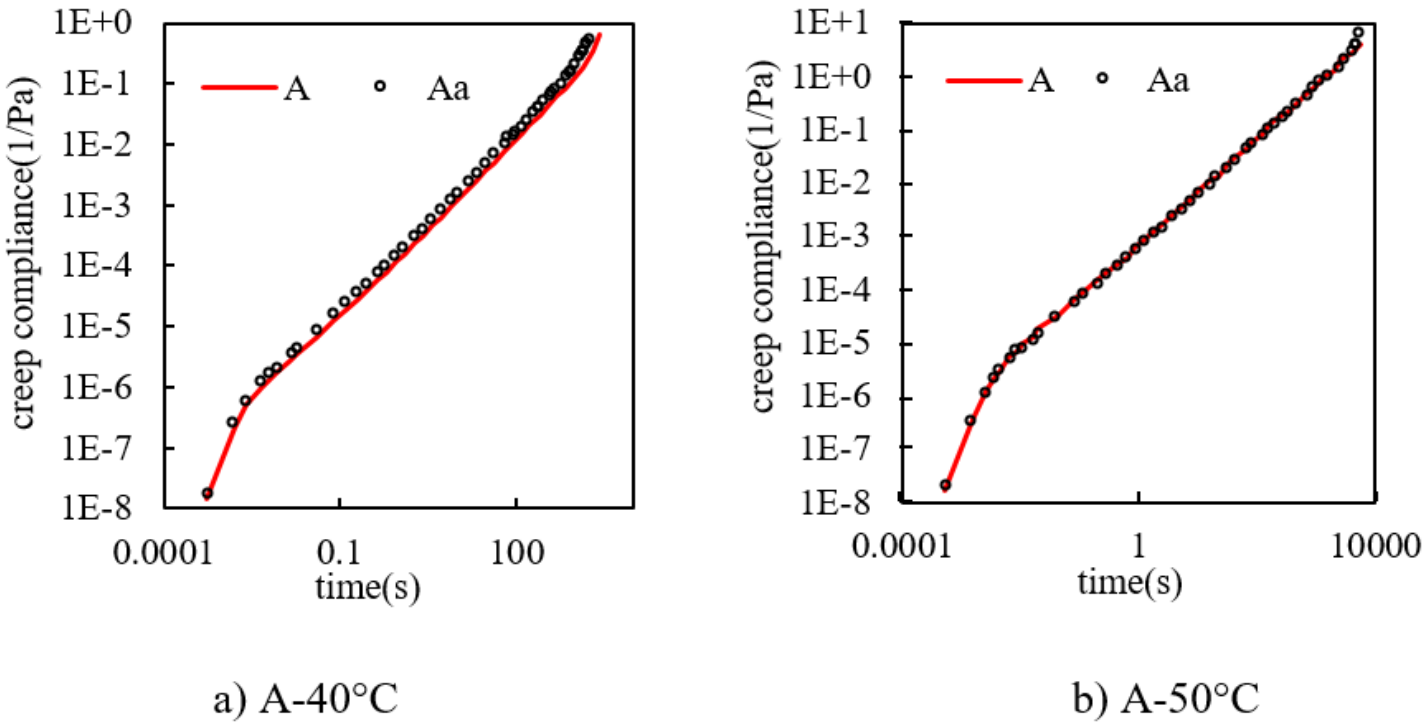

Figure 3

The double-logarithmic curves of creep compliance versus time for conventional creep test and multistage creep test.

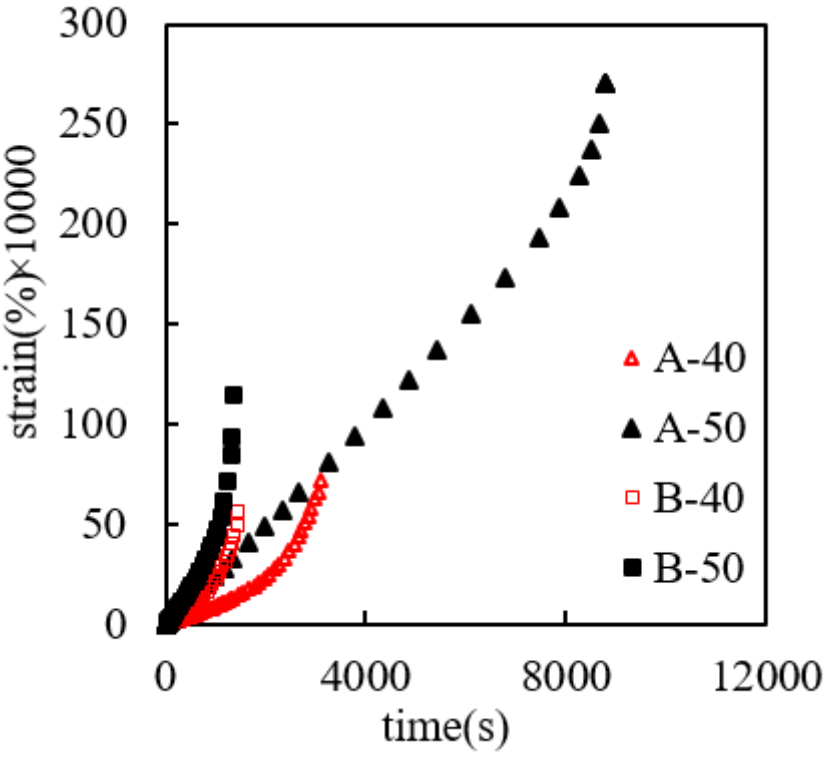

Figure 4

The curves of strain versus time for two asphalt binders.

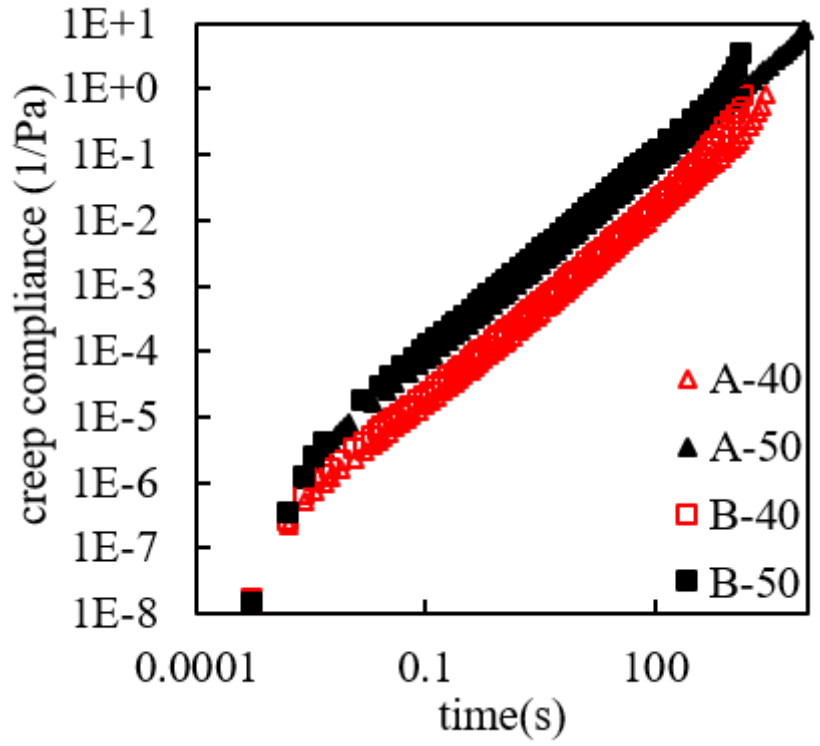

Figure 5

The double-logarithmic curves of creep compliance versus time for two asphalt binders

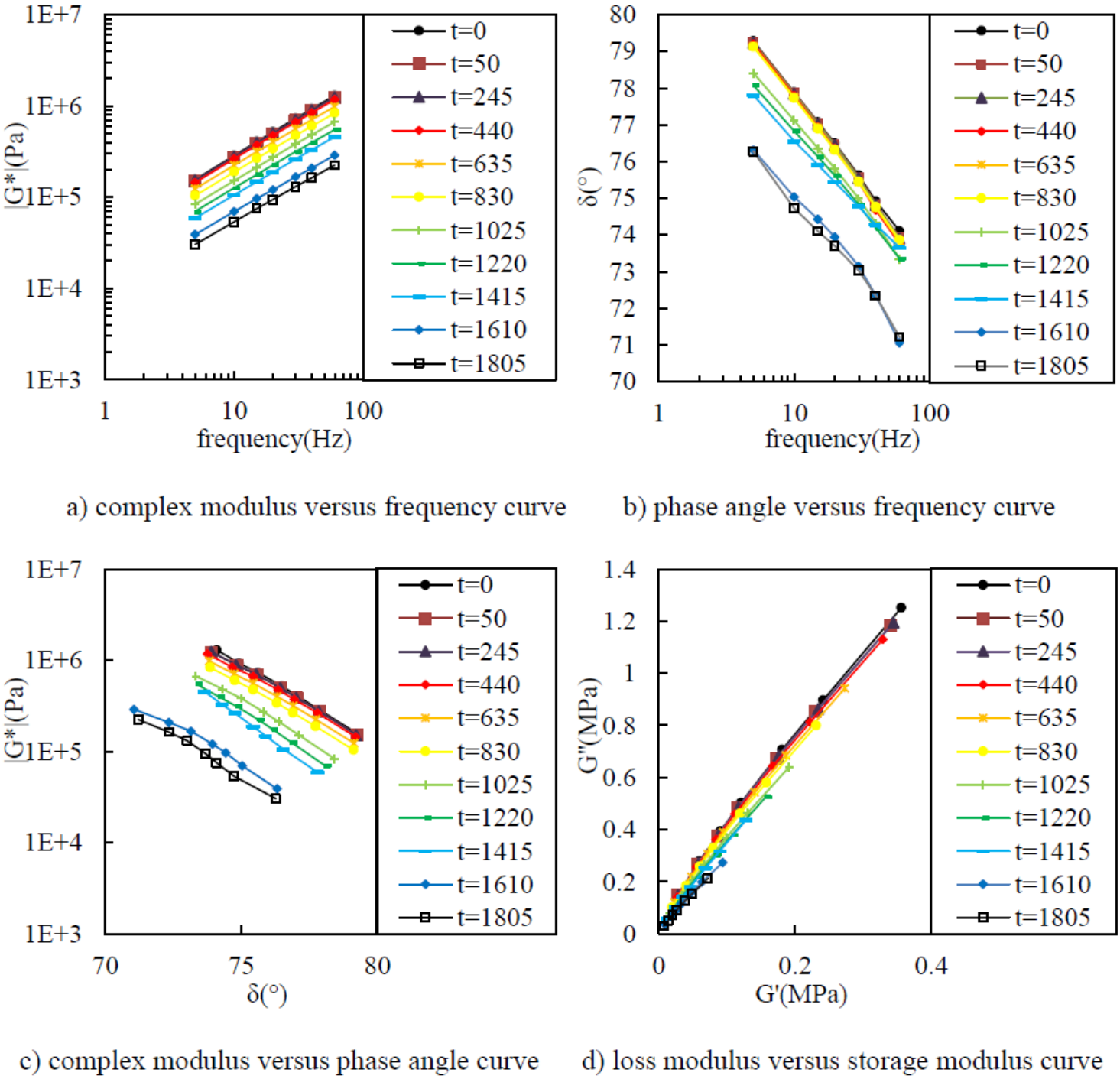

a) complex modulus versus frequency curve

b) phase angle versus frequency curve

c) complex modulus versus phase angle curve

d) loss modulus versus storage modulus curve

Figure 6

The curve clusters of viscoelastic parameters of binder A at 40°C

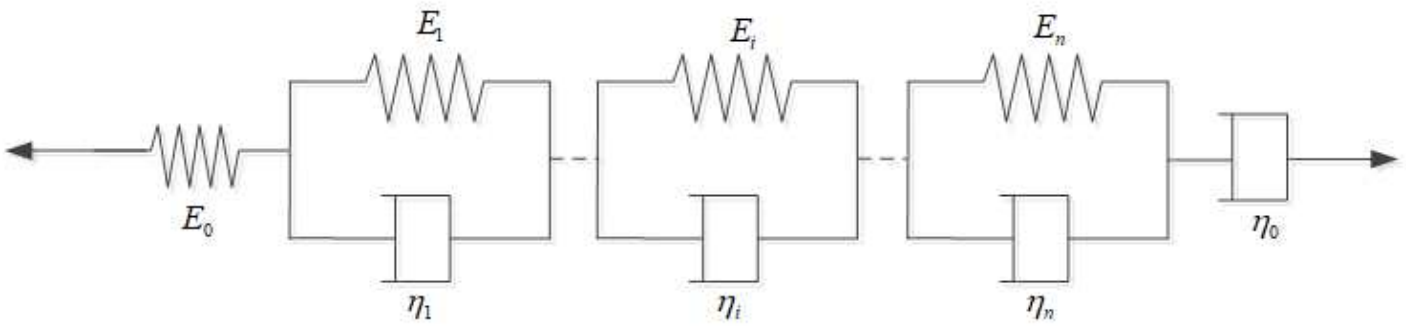

Figure 7

Representation of Generalized Kelvin-Voigt model

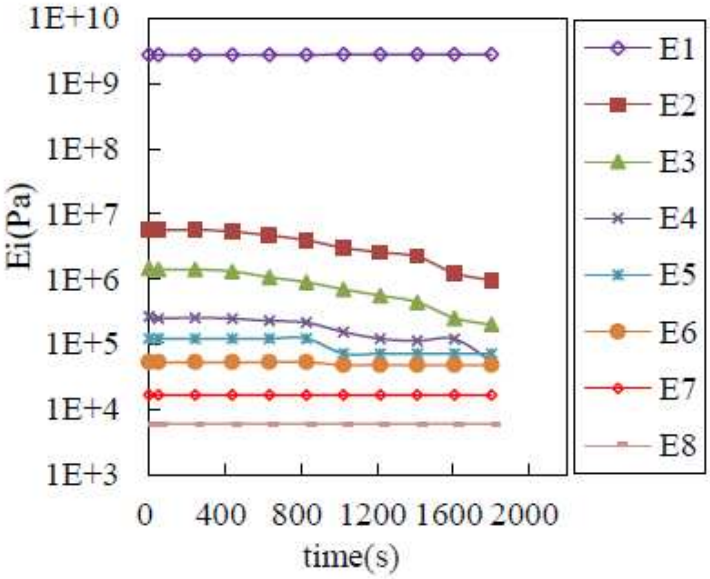

(a) E_i plotted as a function of the loading time

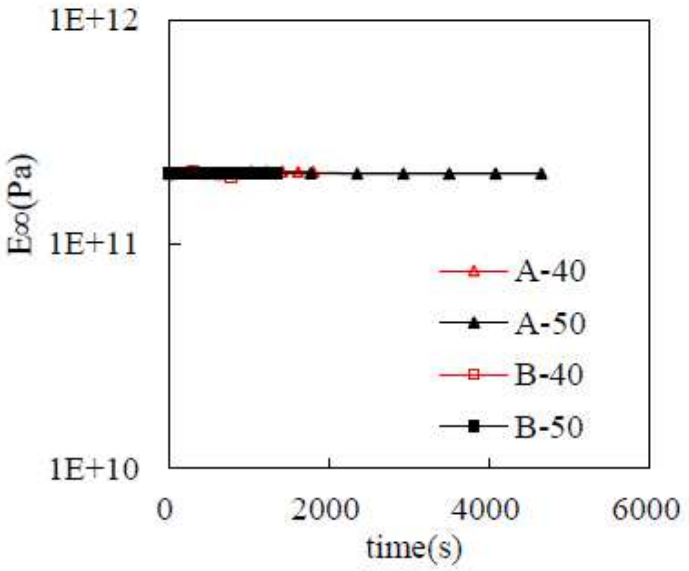

(b) E_∞ plotted as a function of the loading time

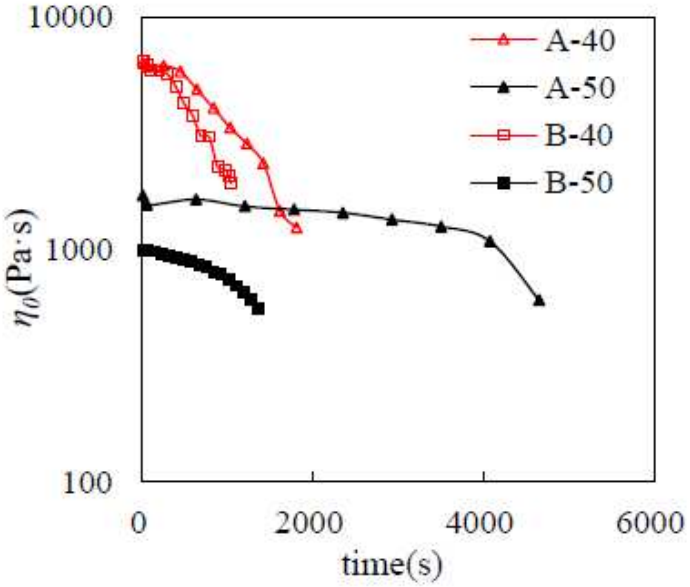

(c) η_0 plotted as a function of the loading time

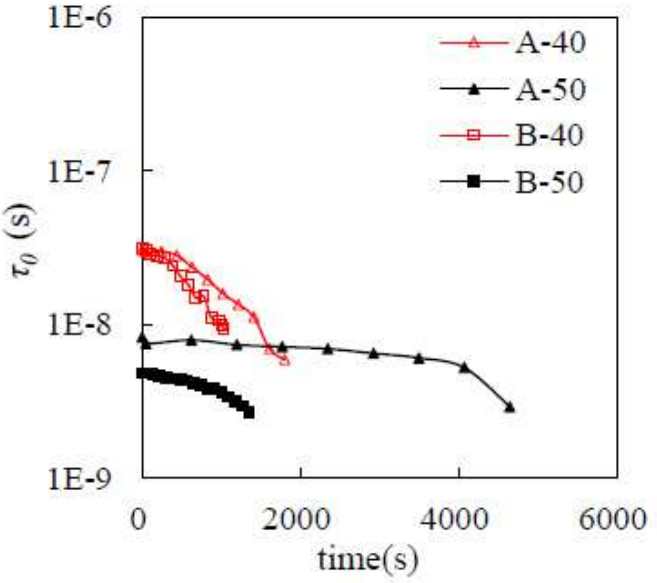

(d) τ_0 plotted as a function of the loading time

Figure 8

Parameters of the generalized Kelvin-Voigt model plotted as a function of the loading time during multi-stage creep test of binder A at 40℃.

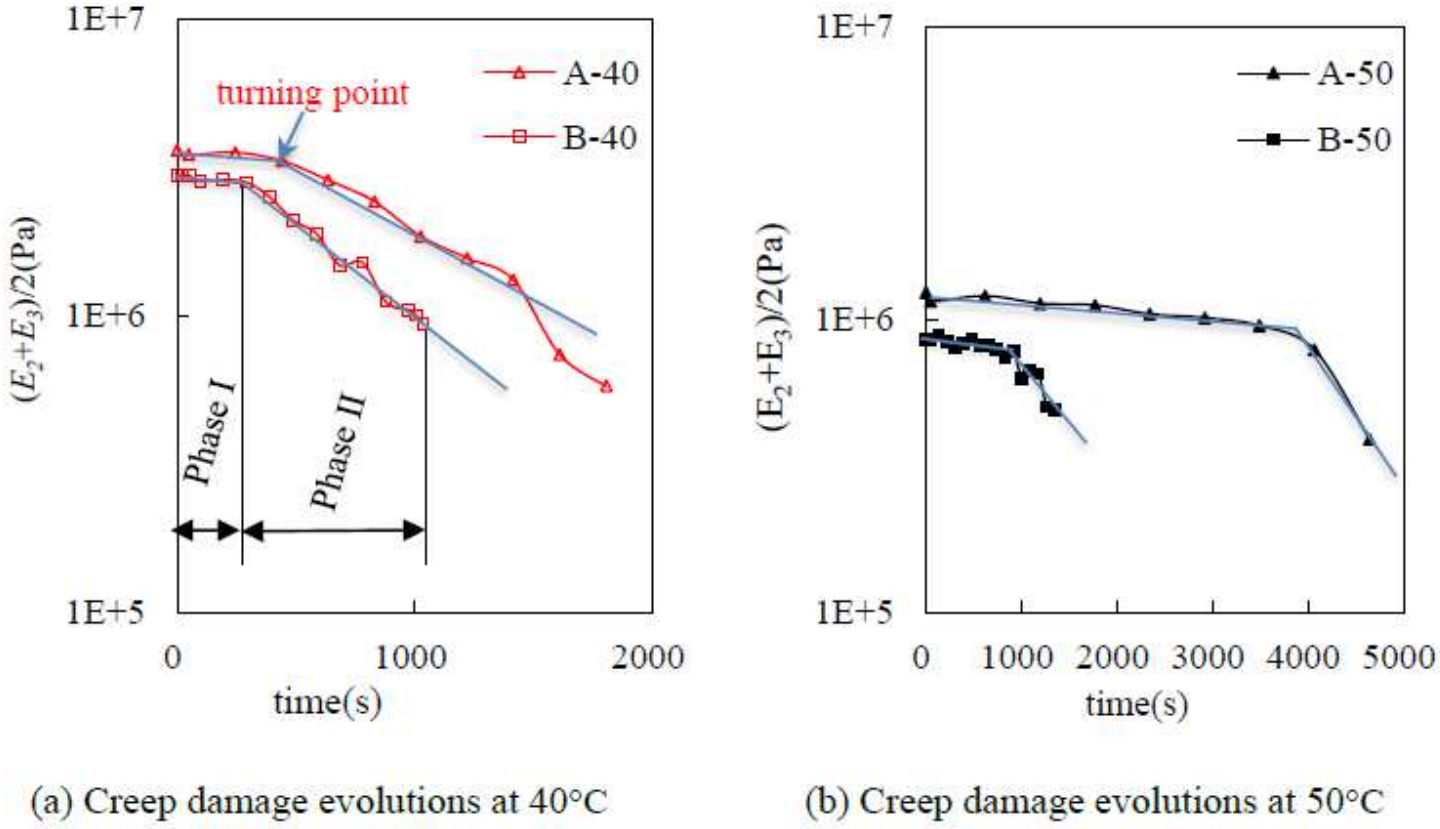

Figure 9

Damage parameter (E2 + E3)/2 plotted as the function of loading time during multi-creep test